Unconventional anomalous Hall effect in a triangular lattice antiferromagnet

Mori Watanabe,[1,*] Tomo Higashihara,[1] Ryotaro Asama,[1] Masashi Tokuda,[1] Shota Suzuki,[1] Nan Jiang,[1,2,3] Masayuki Ochi,[1,4] Hiroaki Ishizuka,[5] Hiroyuki K. Yoshida,[6] and Yasuhiro Niimi[1,2,3,†]

[1]*Department of Physics, Graduate School of Science, Osaka University, Toyonaka, Osaka 560-0043, Japan*
[2]*Center for Spintronics Research Network, Osaka University, Toyonaka, Osaka 560-8531, Japan*
[3]*Institute for Open and Transdisciplinary Research Initiatives, Osaka University, Suita, Osaka 565-0871, Japan*
[4]*Forefront Research Center, Osaka University, Toyonaka, Osaka 560-0043, Japan*
[5]*Department of Physics, Tokyo Institute of Technology, Meguro, Tokyo 152-8551, Japan*
[6]*Department of Physics, Faculty of Science, Hokkaido University, Sapporo, Hokkaido 060-0810, Japan*

(Received 1 March 2024; revised 1 July 2024; accepted 3 July 2024; published 26 July 2024)

We studied the electrical transport properties of a classical spin triangular lattice antiferromagnet Ag_2CrO_2. In this material, a unique spin structure with a five-sublattice unit cell emerges below the Néel temperature T_N, owing to frustration from strong further-neighbor interactions. The material also exhibits unique electrical transport properties coupled with its magnetism, due to a highly conductive layer of Ag_2. Here, we report magnetoresistance and the Hall effect in Ag_2CrO_2 flake devices below and above T_N up to a magnetic field of 8 T. A large magnetoresistance and anomalous Hall effect were observed in the vicinity of T_N, indicating that the fluctuation of the magnetic moments plays a key role. We propose possible scenarios in which the anomalous Hall effect is enhanced through thermal fluctuation.

DOI: 10.1103/PhysRevB.110.024431

I. INTRODUCTION

The anomalous Hall effect (AHE) is the effect in which the measured resistivity transverse to the applied current is enhanced proportionally to the magnetization of the material. First proposed by Karplus and Luttinger [1], and independently proposed by Smit [2,3], it has been widely accepted that the main mechanisms of AHE can be attributed to two origins: the intrinsic and extrinsic scatterings [4]. The former is based on an "anomalous velocity" of the conduction electrons arising from the Berry curvature and originates from the intrinsic band structure of the material, while the latter is an asymmetric scattering at impurities within the material. The interplay of these mechanisms gives rise to a unique scaling relation of the anomalous Hall conductivity σ_{xy} against the longitudinal conductivity σ_{xx}. Such a scaling law has been successful in uncovering the detailed physics of AHE among a plethora of magnetic materials [5].

In recent years, not only research on the above scaling relation but also the search for materials which do not follow the conventional mechanisms have been actively conducted [6–12]. Such materials lead to a further detailed understanding of AHE, and give us a hint to surpass the limit of σ_{xy} set by conventional mechanisms. Such unconventional AHEs are often observed in materials where some exotic spin structure is strongly coupled to the conduction electrons. While theoretical proposals are actively being made to elucidate the details of these effects [13–18], continued electrical transport studies of exotic magnetic systems are important to provide further insight to the phenomena [19,20].

In the present paper, we have focused on an atomically layered frustrated antiferromagnet Ag_2CrO_2 [21]. This material exhibits a unique magnetic ordering due to frustration from strong further-neighbor interactions and geometrical frustration. Below the Néel temperature $T_N \approx 24$ K, Ag_2CrO_2 has a unique magnetic ordering with a five-sublattice magnetic unit cell, where the $S = 3/2$ spins at the Cr^{3+} sites show a strong Ising anisotropy. Although the details of this magnetic state are still a topic of active debate, the most likely magnetic structure is the partially disordered (PD) structure, where one in five spin sites is known to remain as an effective free spin even under its antiferromagnetic order [22,23]. In this magnetic state, a minuscule but finite magnetization hysteresis is observed at 0.5 T, and the magnetization shows a plateau of $\sim 0.4\mu_B/Cr^{3+}$ under an applied magnetic field of 8 T which may indicate the presence of some unsaturated moments at the PD spin sites even under high magnetic fields [24].

Despite these unique properties, experiments on the electronic properties of this material had been limited due to the fact that the bulk material is inherently polycrystalline. We have recently reported the successful fabrication of nearly single-crystalline samples using the mechanical exfoliation technique, which allows us to probe the electronic properties of high-quality Ag_2CrO_2 through nanofabrication [25]. Not only does this method enable us to investigate the anisotropy in the magnetotransport with respect to the crystallographic axis, but also it enables us to access the magnetotransport effects of highly conducting triangular antiferromagnets. We have already reported unique effects found even at the low magnetic field regime, such as the butterfly-shaped magnetoresistance (MR) observed in the field range of <1 T

*Contact author: watanabe@meso.phys.sci.osaka-u.ac.jp
†Contact author: niimi@phys.sci.osaka-u.ac.jp

[26]. This is thought to be caused by the large fluctuations and switching of the PD magnetic moments which is consistent with the magnetization hysteresis, and suggests the large interplay between the magnetic state and the conduction electrons. Thus, it is interesting to consider whether further unique phenomena could be observed in the high-field regime, where the unsaturated magnetic moments are still present. In this paper, we measured the MR and Hall effect in Ag_2CrO_2 flake devices up to 8 T in the temperature range from 5 to 44 K, in order to obtain further information on the electrical transport and magnetic properties. In addition to a large negative MR near T_N, an AHE is induced only in the vicinity of T_N. These results imply that fluctuations of the magnetic moments play a key role in the generation of the observed AHE. Therefore, we propose and discuss possible scenarios in which the fluctuations of the magnetic moments may lead to such behavior, such as the fluctuation-enhanced skew scattering mechanism or spin scalar chirality formed by a noncoplanar spin structure.

II. EXPERIMENTAL DETAILS

The bulk Ag_2CrO_2 crystal was fabricated through a solid-state reaction of Ag, Ag_2O, and Cr_2O_3 powders, which were encapsulated in gold cells and heated at 1200 °C for 1 h under 6 GPa. Although the bulk crystal is inherently polycrystalline, nearly single-crystalline flakes can be extracted through the mechanical exfoliation technique using scotch tape. The flakes were transferred onto 5×5 mm^2 Si/SiO_2 substrates, and Ti/Au electrodes were deposited through electron beam and resistance heating depositions. In the present work, we have measured three samples which we label sample A (thickness 200 nm, length 4.5 μm, width 2.6 μm), B (thickness 200 nm, length 3.7 μm, width 1.6 μm), and C (thickness 60 nm, length 4.1 μm, width 1.8 μm). Otherwise stated, the data shown in the following sections are the measurement of sample A.

The devices were cooled using a variable temperature insert with a superconducting magnet, and electrical transport measurements were performed using the standard four-probe method through a commercial lock-in amplifier SR830. As mentioned in our previous report, all Ag_2CrO_2 flakes are deposited onto the substrate with the *c* axis perpendicular to the basal plane [25]. Therefore, the applied current directions were along the *a*-*b* plane for all samples, and the applied current densities were 1.9×10^5, 1.6×10^5, and 4.6×10^5 A/cm^2 for samples A, B, and C, respectively. As mentioned in the Supplemental Material Sec. IV A [27], Joule heating should not play a major role in our measurement setup due to the low resistance of the flake devices.

III. RESULTS

First, we show the temperature dependence of the resistivity of a typical Ag_2CrO_2 flake device in Fig. 1. As already demonstrated in previous studies, a characteristic drop in the resistivity is observed with the onset of the antiferromagnetic order, which is caused by the large suppression of magnon scattering. The difference from the previous reports is the resistivity at low temperature: It is nearly two orders of magnitude smaller than that of polycrystalline samples. This improvement is due to the fact that the device is of nearly single-crystalline quality. It should be noted that the resistivity of 0.7 μΩ cm at $T = 5$ K is almost the lowest in mesoscopic scale metals, comparable to or even lower than that of pure Au or Ag.

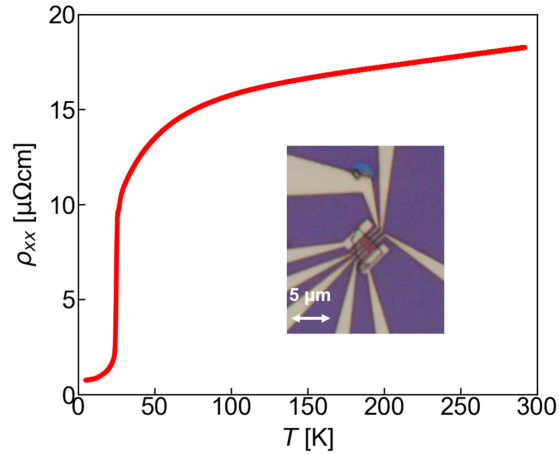

FIG. 1. Electrical resistivity of a typical Ag_2CrO_2 flake device. The inset shows an optical microscope image of the device.

Next, we performed MR and Hall measurements in the temperature range of 5–44 K up to 8 T. In Fig. 2, the longitudinal MR at notable temperatures is displayed. Here, the raw data are shown to clearly display the butterfly-shaped MR. At the lowest measured temperature ($T = 5.4$ K), a large positive MR of +80% was observed. A positive MR well below the transition temperature often occurs in magnetic materials due to the Lorentz force. It usually shows a parabolic field dependence at low temperatures when the electron mean free path is long enough to overcome the negative MR caused by the suppression of spin scattering. Moreover, a positive parabolic MR also occurs when an external magnetic field is applied along the sublattice magnetization axis [36,37]. We believe that both the Lorentz force contribution as well as the antiferromagnetic structure contribute to the emergence of the positive MR. Meanwhile, it is important to note that we observed a nonparabolic field dependence in the low-temperature regime, which cannot be explained by the above two origins. Further investigations such as the in-plane magnetic field dependence are required to elucidate this effect. As the temperature is increased, the emergence of the negative MR is observed, which does not saturate up to 8 T in the case of $T = 24.6$ K. Such behaviors are observed in ferromagnetic materials, where the fluctuations of the magnetic moments near its transition temperature induce spin scattering, and are suppressed with the application of the external field, leading to a decrease in the magnetic scattering [38,39]. In this case, we believe the negative MR arises from the PD moments which are most likely to be ferromagnetically coupled along the *c* axis.

The negative MR takes a maximum absolute value of 65% in the vicinity of T_N, suggesting that the fluctuations of the magnetic moments are largest in this temperature range. It is also striking that the maximum MR ratio difference of roughly 140% is achieved between 5 and 24 K due to the large positive and negative MR, which emphasizes that the

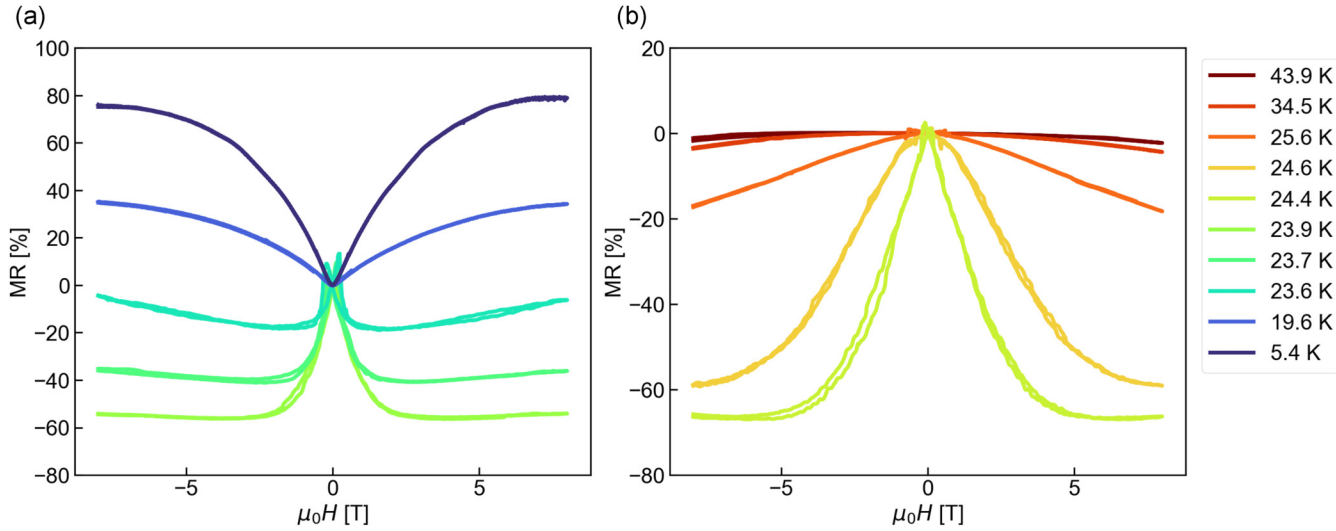

FIG. 2. Magnetoresistance (MR) ratio (a) below and (b) above T_N at notable temperatures. The magnetic field is applied along the stacking direction of the material.

magnetic structure has a significant effect on the electronic properties in Ag_2CrO_2.

The Hall resistance of Ag_2CrO_2 was taken simultaneously with the MR. In Fig. 3(a), we show the Hall resistivity ρ_H as a function of the perpendicular magnetic field at notable temperatures. Since the raw data contain some longitudinal component, the asymmetric component of the raw data is taken as ρ_H and plotted in Fig. 3(a). No significant hysteresis was observed in our Hall measurement throughout the entire temperature range. The carrier type is an electron, which is consistent with the previous studies where the Ag 5*s* band provides the conduction carriers in Ag_2MO_2 (M = magnetic ion) materials [40–42]. Along with the ordinary Hall effect, some nonlinear component was observed in the temperature range close to T_N. First, the ordinary Hall component was analyzed through a linear fit above 6 T, where the magnetization of the bulk material roughly plateaus. Assuming a single carrier model, the electron carrier concentration was estimated as 0.9–1.5 $\times$ 10^{22} cm^{-3}, which is in the same order of magnitude as the carrier concentration of Ag (5–6 $\times$ 10^{22} cm^{-3}). Making use of the effective electron mass obtained from the zero-field longitudinal resistivity, the temperature dependence of the electron mobility can also be obtained, as shown in Fig. 3(b). Similar to the large drop in the resistivity at T_N, an enhancement in the mobility by a factor of roughly 4 is observed between $T = 23.1$ and 25.7 K. This is further supportive evidence of large fluctuations of magnetic moments which are suppressed below T_N, leading to a notable increase in the mobility. The maximum value of the mobility in Ag_2CrO_2 exceeds 1080 $cm^2/V\,s$, which is comparable to crystalline silicon at room temperature of roughly 1400 $cm^2/V\,s$ [43].

Now we analyze the anomalous Hall component defined as ρ_{AHE}, by subtracting the ordinary Hall effect from ρ_H, which is shown in Fig. 4(a) for notable temperatures. While the anomalous Hall contributions from the magnetization hysteresis around 0.5 T were minuscule (Supplemental Material Sec. IV B [27]), a saturation of the anomalous component

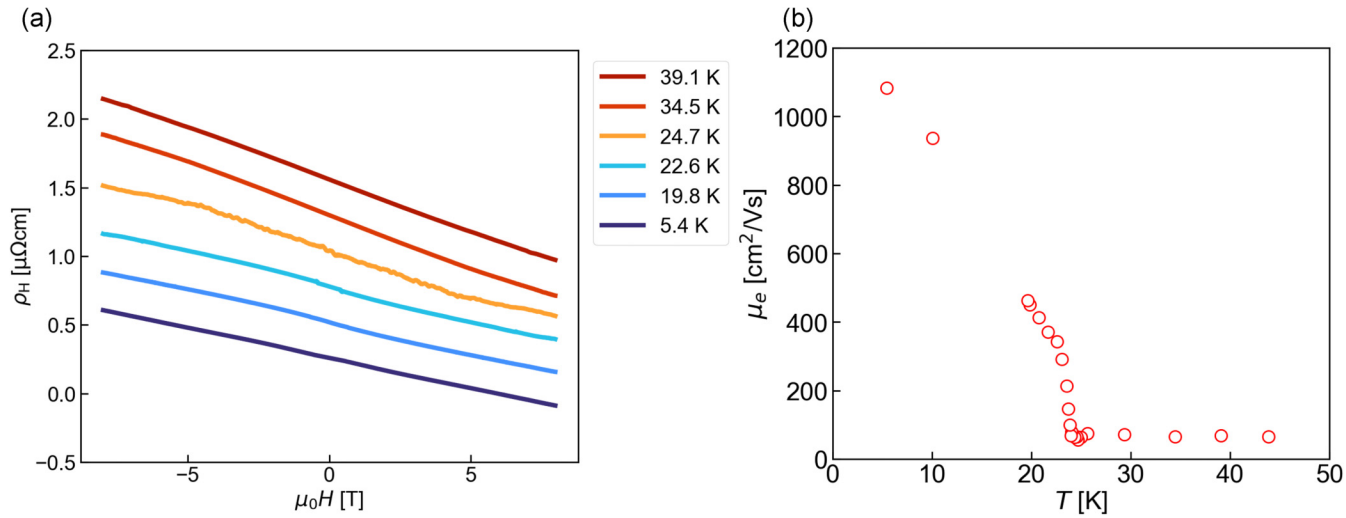

FIG. 3. (a) Hall resistivity ρ_H at notable temperatures. (b) Electron mobility obtained from the linear fit at high fields.

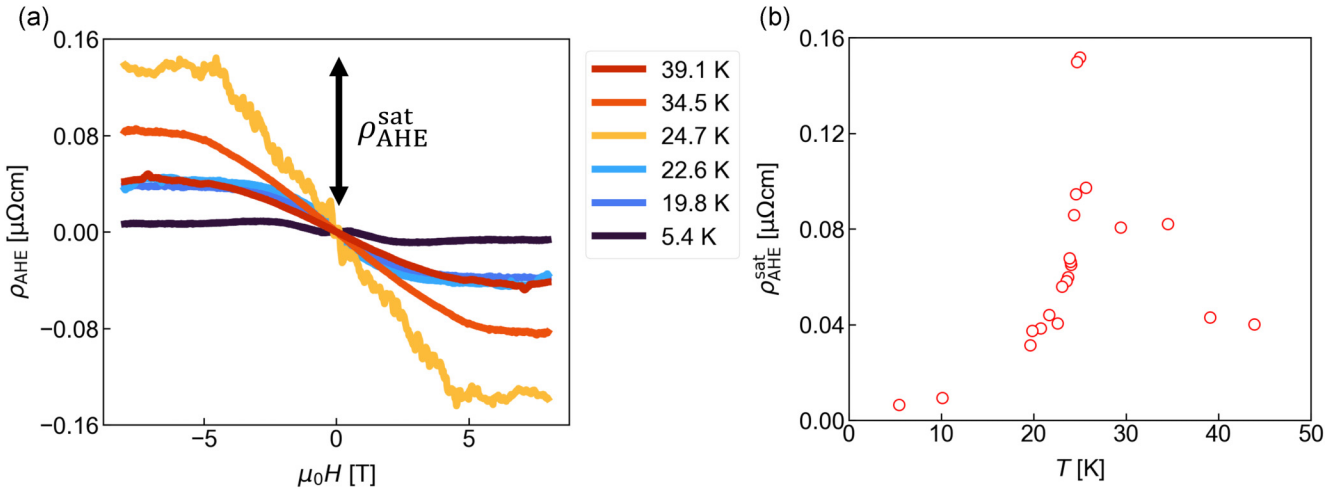

FIG. 4. (a) Anomalous component of the Hall resistivity ρ_{AHE} at notable temperatures, with the definition of ρ_{AHE}^{sat}. (b) Temperature dependence of ρ_{AHE}^{sat}.

was observed for fields above 5 T. Figure 4(b) shows the temperature dependence of ρ_{AHE}^{sat}, which has a sharp peak in the vicinity of T_N. This is clearly different from the behavior of the bulk magnetization, which shows a small but finite hysteresis loop below $T = 20$ K. This behavior is also unlikely to be a multicarrier effect because it is notable only at the vicinity of T_N. Since the longitudinal resistivity changes drastically within this temperature range as shown in Fig. 1, we show the temperature dependence of the AHE angle $\tan\theta_{AHE} = \rho_{AHE}^{sat}/\rho_{xx}$ in Fig. 5(a). The striking result is the fact that $\tan\theta_{AHE}$ takes a maximum value of 2%–4%, depending on the sample quality. As the difference in sample quality leads to changes in the longitudinal resistivity, we have plotted the scaling relation between σ_{AHE} and σ_{xx} from 40 to 20 K where the Hall angle shows the unique temperature dependence. This is shown in Fig. 5(b). The nonlinear AHE behavior was consistent throughout all the measured samples (Supplemental Material Sec. IV C [27]), and σ_{AHE} shows a clear σ_{xx} dependence throughout all the measured samples. The scaling relation follows roughly $\alpha \sim 1.75$ for $\sigma_{AHE} \propto \sigma_{xx}^{\alpha}$, and such σ_{xx} dependence of σ_{AHE} is observed even in regimes where the intrinsic mechanism should dominate.

IV. DISCUSSION

We now discuss the possible origin of the unconventional Hall effect. For this purpose, we performed first-principles calculations for Ag_2CrO_2, in order to gain information on the electronic structure and hybridization of Ag and Cr orbitals (Supplemental Material Sec. I [27]). The calculated band dispersion [Figs. S1(a)–S1(d)] shows that the dispersive Ag-*s* band crosses the Fermi energy, which likely dominates the electrical transport, as is consistent with previous results. We also calculated the density of states (DOS) for the low-temperature structure with the PD magnetic state. As shown in Figs. S1(e) and S1(f), whether the Cr-*d* partial DOS remains near the Fermi energy strongly depend on the Hubbard-U correction, which is 0 and 3 eV for Figs. S1(e) and S1(f), respectively. In general, it is difficult to evaluate an appropriate U value for the band-structure calculation.

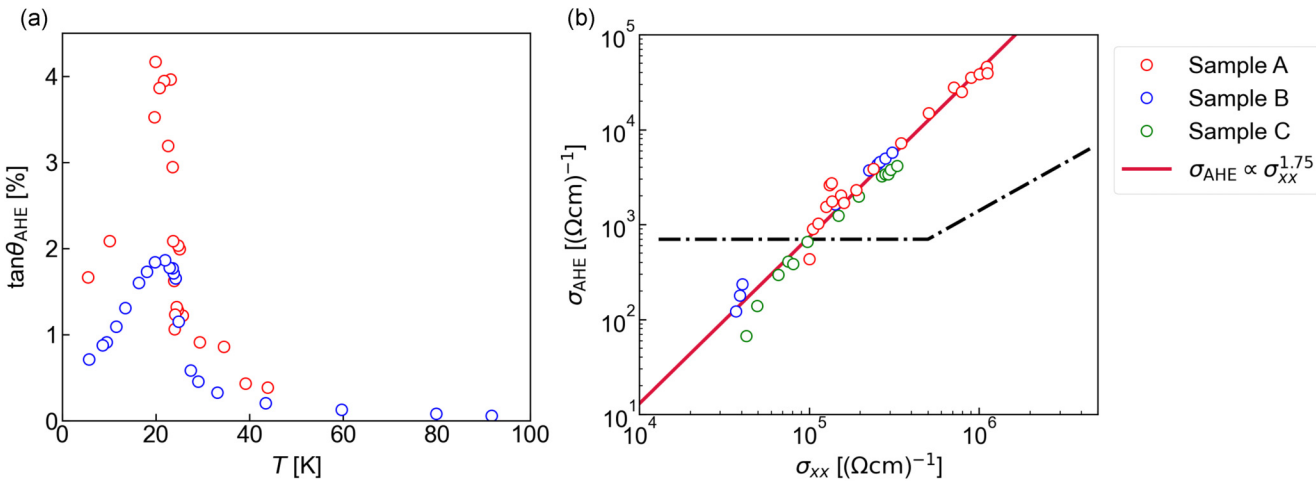

FIG. 5. (a) Temperature dependence of the AHE angle $\tan\theta_{AHE}$. (b) Scaling relation between the longitudinal resistivity σ_{xx} and σ_{AHE} in the temperature range from 40 to 20 K. The guide to the eye (dotted line) indicates the conventional scaling relation seen in magnetic materials.

We believe that the real electronic structure lies somewhere in between the two calculations. This is also consistent with previous experimental reports; the Sommerfeld constant for the polycrystalline bulk was given as 9.74 $\mathrm{mJ/mol\,K^2}$ [21], implying a heavy effective electron mass, while the magnetic moment of the ordered Cr sites showed an almost full saturation of $2.9(1)\mu_B$ [44], indicating an almost full saturation for $S = 3/2$. These two experimental results suggest that there is a finite DOS of the Cr-d bands at the Fermi energy, meanwhile the DOS may also be relatively small due to the almost fully occupied t_{2g}^3 state.

Given these band-calculation analyses, we return to the temperature dependence of the AHE angle. As the AHE is maximized at the magnetic transition, it is likely that the effect originates from the fluctuations of the PD moments near T_N. As far as we know, there are two main mechanisms where the thermal fluctuations of the magnetic moments can give rise to an enhancement of the AHE. One is the skew scattering enhancement due to thermal fluctuations presented by Kondo [45], and the other is the scalar spin chirality model [14–18]. Both of these effects can arise from extrinsic mechanisms, which is consistent with our scaling plot which showed a strong σ_{xx} dependence of the AH conductivity. In the following, we will discuss the feasibility of each mechanism.

As for the Kondo mechanism, the AHE originates from the s-d interaction in a magnetic material. With consideration of the higher-order terms in the Born approximation, Kondo showed that the skew scattering of a magnetic material can be enhanced near the magnetic transition temperature. This effect is observed in clean ferromagnetic materials such as Fe or Ni, and has been successful in addressing their AHE temperature dependence. In our case, such a scenario could occur if hybridization between the Ag-s band and the Cr-d band exists, which could then explain the temperature dependence of the AHE angle in our data. However, the Kondo mechanism is not enough to explain the magnitude of the AHE angle observed in our experiment. This is due to the small partial DOS of the Cr-d band at the Fermi level stated earlier, from which a relatively weak s-d interaction is expected. Considering the fact that a maximum AHE angle of only 0.1% is observed even for clean ferromagnets such as Fe [12,46], an AHE angle of a few percent would not be due to the skew scattering mechanism presented by Kondo, especially when the hybridization of Ag-Cr bands may be weak.

Meanwhile, several kagome lattice materials have been reported to possess unconventionally large AHE angles of few tens of percent, owing to the scalar spin chirality obtained by the noncoplanar magnetic structure [12,19]. In the spin scalar chirality mechanism, a noncoplanar spin structure can lead to a finite Berry curvature, resulting in an AHE which is not simply proportional to the magnetization. It has also been shown theoretically that the skew scattering due to the noncoplanar structure can be greatly enhanced with the aid of thermal fluctuations of the magnetic moments [47]. Therefore, the temperature dependence of the AHE and the magnitude of the AHE angle could also be explained if there exists some noncoplanar structure in our system. It should also be noted that the AHE observed in Ag_2CrO_2 possesses a unique magnetic field dependence, in which a saturation of the AHE is observed before the saturation of the MR. This could also be explained if the AHE originates from a noncoplanar structure (Supplemental Material Sec. III [27]). However, the problem in this scenario lies in the determination of the magnetic structure which possesses such scalar spin chirality. For example, a finite scalar spin chirality cannot be obtained by calculations from the two-dimensional Ising spin model proposed by Takagi *et al.* [48], as detailed in Supplemental Material Sec. II [27]. It is important to note that there were some discrepancies between the simulation results and the actual data, such as the external field dependence of the magnetization, leading us to believe that the two-dimensional PD model may not be a suitable effective model to elucidate the origin of our results. In order to fully explain the observed phenomena, further refinements of the PD model may be required, such as the inclusion of canting of the ordered moments or expansion of the model to three dimensions, or consideration of other mechanisms rather than the two presented in the current paper may be required.

V. CONCLUSIONS

In conclusion, we have measured the magnetoresistance and Hall effect of the triangular lattice antiferromagnet Ag_2CrO_2. In the magnetoresistance measurement, a large positive magnetoresistance was observed, possibly related to the antiferromagnetic structure. Near the Néel temperature $T_N \approx 24$ K, a substantially large negative magnetoresistance was observed, which does not saturate up to high magnetic fields. This indicates large fluctuations of the magnetic moments at this temperature. In the same temperature range, a nonlinear component in the Hall effect was observed. The obtained Hall angle $\tan\theta_{AHE}$ reaches 4%, and its scaling relation with respect to the longitudinal conductivity indicates that this effect arises from extrinsic scattering mechanisms. It is strongly indicated that the fluctuating moment near T_N plays a key role in the unique AHE, although further research on the PD structure is required to fully elucidate the origin. The result is one of the few experimental reports on the electrical transport of metallic triangular lattice magnetic systems, and demonstrates the unique magnetotransport properties arising from conduction electrons which are coupled to exotic magnetic structures.

ACKNOWLEDGMENTS

We thank P. Noël, M. Matsuda, S. Hayami, H. Kusunose for the fruitful discussions. This work was supported by JSPS KAKENHI (Grants No. JP20H02557, No. JP21J20477, No. JP22H04481, and No. JP23H00257) and JST FOREST (Grant No. JPMJFR2134).

[1] R. Karplus and J. M. Luttinger, Hall effect in ferromagnetics, Phys. Rev. **95**, 1154 (1954).

[2] J. Smit, The spontaneous Hall effect in ferromagnetics I, Physica **21**, 877 (1955).

[3] J. Smit, The spontaneous Hall effect in ferromagnetics II, Physica **24**, 39 (1958).

[4] N. Nagaosa, J. Sinova, S. Onoda, A. H. MacDonald, and N. P. Ong, Anomalous Hall effect, Rev. Mod. Phys. **82**, 1539 (2010).

[5] S. Onoda, N. Sugimoto, and N. Nagaosa, Quantum transport theory of anomalous electric, thermoelectric, and thermal Hall effects in ferromagnets, Phys. Rev. B **77**, 165103 (2008).

[6] Y. Taguchi, Y. Oohara, H. Yoshizawa, N. Nagaosa, and Y. Tokura, Spin chirality, Berry phase, and anomalous Hall effect in a frustrated ferromagnet, Science **291**, 2573 (2001).

[7] Y. Machida, S. Nakatsuji, Y. Maeno, T. Tayama, T. Sakakibara, and S. Onoda, Unconventional anomalous Hall effect enhanced by a noncoplanar spin texture in the frustrated Kondo lattice $Pr_2Ir_2O_7$, Phys. Rev. Lett. **98**, 057203 (2007).

[8] L. A. Fenner, A. A. Dee, and A. S. Wills, Non-collinearity and spin frustration in the itinerant kagome ferromagnet Fe_3Sn_2, J. Phys.: Condens. Matter **21**, 452202 (2009).

[9] T. Kida, L. A. Fenner, A. A. Dee, I. Terasaki, M. Hagiwara, and A. S. Wills, The giant anomalous Hall effect in the ferromagnet Fe_3Sn_2—a frustrated kagome metal, J. Phys.: Condens. Matter **23**, 112205 (2011).

[10] H. Takatsu, S. Yonezawa, S. Fujimoto, and Y. Maeno, Unconventional anomalous Hall effect in the metallic triangular-lattice magnet $PdCrO_2$, Phys. Rev. Lett. **105**, 137201 (2010).

[11] S. S. Sunku, T. Kong, T. Ito, P. C. Canfield, B. S. Shastry, P. Sengupta, and C. Panagopoulos, Hysteretic magnetoresistance and unconventional anomalous Hall effect in the frustrated magnet TmB_4, Phys. Rev. B **93**, 174408 (2016).

[12] S.-Y. Yang, Y. Wang, B. R. Ortiz, D. Liu, J. Gayles, E. Derunova, R. Gonzalez-Hernandez, L. Šmejkal, Y. Chen, S. S. P. Parkin, S. D. Wilson, E. S. Toberer, T. McQueen, and M. N. Ali, Giant, unconventional anomalous Hall effect in the metallic frustrated magnet candidate, KV_3Sb_5, Sci. Adv. **6**, eabb6003 (2020).

[13] N. Nagaosa, Anomalous Hall effect—a new perspective, J. Phys. Soc. Jpn. **75**, 042001 (2006).

[14] J. Ye, Y. B. Kim, A. J. Millis, B. I. Shraiman, P. Majumdar, and Z. Tešanović, Berry phase theory of the anomalous Hall effect: Application to colossal magnetoresistance manganites, Phys. Rev. Lett. **83**, 3737 (1999).

[15] Y. Lyanda-Geller, S. H. Chun, M. B. Salamon, P. M. Goldbart, P. D. Han, Y. Tomioka, A. Asamitsu, and Y. Tokura, Charge transport in manganites: Hopping conduction, the anomalous Hall effect, and universal scaling, Phys. Rev. B **63**, 184426 (2001).

[16] G. Tatara and H. Kawamura, Chirality-driven anomalous Hall effect in weak coupling regime, J. Phys. Soc. Jpn. **71**, 2613 (2002).

[17] H. Kawamura, Spin-chirality decoupling in Heisenberg spin glasses and related systems, J. Magn. Magn. Mater. **310**, 1487 (2007).

[18] H. Ishizuka and N. Nagaosa, Large anomalous Hall effect and spin Hall effect by spin-cluster scattering in the strong-coupling limit, Phys. Rev. B **103**, 235148 (2021).

[19] Y. Fujishiro, N. Kanazawa, R. Kurihara, H. Ishizuka, T. Hori, F. S. Yasin, X. Yu, A. Tsukazaki, M. Ichikawa, M. Kawasaki, N. Nagaosa, M. Tokunaga, and Y. Tokura, Giant anomalous Hall effect from spin-chirality scattering in a chiral magnet, Nat. Commun. **12**, 317 (2021).

[20] X. Wang and J. Tan, Switching from extrinsic to intrinsic anomalous Hall effect around Lifshitz transition in a Kagome-lattice ferromagnet, Appl. Phys. Lett. **122**, 051901 (2023).

[21] H. Yoshida, E. Takayama-Muromachi, and M. Isobe, Novel $S = 3/2$ triangular antiferromagnet Ag_2CrO_2 with metallic conductivity, J. Phys. Soc. Jpn. **80**, 123703 (2011).

[22] J. Sugiyama, H. Nozaki, K. Miwa, H. Yoshida, M. Isobe, K. Prša, A. Amato, D. Andreica, and M. Månsson, Partially disordered spin structure in Ag_2CrO_2 studied with μ^+SR, Phys. Rev. B **88**, 184417 (2013).

[23] M. Matsuda, S. E. Dissanayake, H. K. Yoshida, M. Isobe, and M. B. Stone, Magnetic excitations affected by spin-lattice coupling in the $S = \frac{3}{2}$ triangular lattice antiferromagnet Ag_2CrO_2, Phys. Rev. B **102**, 214411 (2020).

[24] T. Kida, A. Okutani, H. Yoshida, and M. Hagiwara, Transport properties of the metallic two-dimensional triangular antiferromagnet Ag_2CrO_2, Phys. Procedia **75**, 647 (2015).

[25] H. Taniguchi, S. Suzuki, T. Arakawa, H. Yoshida, Y. Niimi, and K. Kobayashi, Fabrication of thin films of two-dimensional triangular antiferromagnet Ag_2CrO_2 and their transport properties, AIP Adv. **8**, 025010 (2018).

[26] H. Taniguchi, M. Watanabe, M. Tokuda, S. Suzuki, E. Imada, T. Ibe, T. Arakawa, H. Yoshida, H. Ishizuka, K. Kobayashi, and Y. Niimi, Butterfly-shaped magnetoresistance in triangular-lattice antiferromagnet Ag_2CrO_2, Sci. Rep. **10**, 2525 (2020).

[27] See Supplemental Material at http://link.aps.org/supplemental/10.1103/PhysRevB.110.024431 for (I) the DFT calculations performed for the Ag_2CrO_2 band structure, (II) the scalar spin chirality analysis for the five partially disordered state, (III) the discussion on the magnetic field dependencies of the magnetoresistance and the anomalous Hall effect, and (IV) additional experimental details performed on samples A, B, and C, which includes Refs. [28–35,44,48].

[28] J. P. Perdew, K. Burke, and M. Ernzerhof, Generalized gradient approximation made simple, Phys. Rev. Lett. **77**, 3865 (1996).

[29] G. Kresse and D. Joubert, From ultrasoft pseudopotentials to the projector augmented-wave method, Phys. Rev. B **59**, 1758 (1999).

[30] G. Kresse and J. Hafner, *Ab initio* molecular dynamics for liquid metals, Phys. Rev. B **47**, 558 (1993).

[31] G. Kresse and J. Hafner, *Ab initio* molecular-dynamics simulation of the liquid-metal–amorphous-semiconductor transition in germanium, Phys. Rev. B **49**, 14251 (1994).

[32] G. Kresse and J. Furthmüller, Efficiency of *ab-initio* total energy calculations for metals and semiconductors using a plane-wave basis set, Comput. Mater. Sci. **6**, 15 (1996).

[33] G. Kresse and J. Furthmüller, Efficient iterative schemes for *ab initio* total-energy calculations using a plane-wave basis set, Phys. Rev. B **54**, 11169 (1996).

[34] A. I. Liechtenstein, V. I. Anisimov, and J. Zaanen, Density-functional theory and strong interactions: Orbital ordering in Mott-Hubbard insulators, Phys. Rev. B **52**, R5467 (1995).

[35] S. L. Dudarev, G. A. Botton, S. Y. Savrasov, C. J. Humphreys, and A. P. Sutton, Electron-energy-loss spectra and the structural stability of nickel oxide: An LSDA+U study, Phys. Rev. B **57**, 1505 (1998).

[36] H. Nagasawa, Magnetoresistance of neodymium metal, Phys. Lett. A **41**, 39 (1972).

[37] H. Yamada and S. Takada, Magnetoresistance of antiferromagnetic metals due to *s*-*d* interaction, J. Phys. Soc. Jpn. **34**, 51 (1973).

[38] H. Yamada and S. Takada, Negative magnetoresistance of ferromagnetic metals due to spin fluctuations, Prog. Theor. Phys. **48**, 1828 (1972).

[39] B. Raquet, M. Viret, E. Sondergard, O. Cespedes, and R. Mamy, Electron-magnon scattering and magnetic resistivity in 3*d* ferromagnets, Phys. Rev. B **66**, 024433 (2002).

[40] H. Yoshida, Y. Muraoka, T. Sörgel, M. Jansen, and Z. Hiroi, Spin-$\frac{1}{2}$ triangular lattice with orbital degeneracy in a metallic oxide Ag_2NiO_2, Phys. Rev. B **73**, 020408(R) (2006).

[41] H. Yoshida, S. Ahlert, M. Jansen, Y. Okamoto, J.-I. Yamaura, and Z. Hiroi, Unique phase transition on spin-2 triangular lattice of Ag_2MnO_2, J. Phys. Soc. Jpn. **77**, 074719 (2008).

[42] U. Wedig, P. Adler, J. Nuss, H. Modrow, and M. Jansen, Studies on the electronic structure of Ag_2NiO_2, an intercalated delafossite containing subvalent silver, Solid State Sci. **8**, 753 (2006).

[43] P. Norton, T. Braggins, and H. Levinstein, Impurity and lattice scattering parameters as determined from Hall and mobility analysis in *n*-type silicon, Phys. Rev. B **8**, 5632 (1973).

[44] M. Matsuda, C. de la Cruz, H. Yoshida, M. Isobe, and R. S. Fishman, Partially disordered state and spin-lattice coupling in an $S = \frac{3}{2}$ triangular lattice antiferromagnet Ag_2CrO_2, Phys. Rev. B **85**, 144407 (2012).

[45] J. Kondo, Anomalous Hall effect and magnetoresistance of ferromagnetic metals, Prog. Theor. Phys. **27**, 772 (1962).

[46] T. Miyasato, N. Abe, T. Fujii, A. Asamitsu, S. Onoda, Y. Onose, N. Nagaosa, and Y. Tokura, Crossover behavior of the anomalous Hall effect and anomalous Nernst effect in itinerant ferromagnets, Phys. Rev. Lett. **99**, 086602 (2007).

[47] S. Onoda and N. Nagaosa, Spin chirality fluctuations and anomalous Hall effect in itinerant ferromagnets, Phys. Rev. Lett. **90**, 196602 (2003).

[48] T. Takagi and M. Mekata, New partially disordered phases with commensurate spin density wave in frustrated triangular lattice, J. Phys. Soc. Jpn. **64**, 4609 (1995).